

## NONTHERMAL CONTINUUM TOWARD SAGITTARIUS B2(N-LMH)

J. M. HOLLIS,<sup>1</sup> P. R. JEWELL,<sup>2</sup> ANTHONY J. REMIJAN,<sup>2</sup> AND F. J. LOVAS<sup>3</sup>

Received 2007 February 6; accepted 2007 March 15; published 2007 April 11

### ABSTRACT

An analysis of continuum antenna temperatures observed in the GBT spectrometer bandpasses is presented for observations toward Sgr B2(N-LMH). Since 2004, we have identified four new prebiotic molecules toward this source by means of rotational transitions between low-energy levels; concurrently, we have observed significant continuum in GBT spectrometer bandpasses centered at 85 different frequencies in the range 1–48 GHz. The continuum heavily influences the molecular spectral features since we have observed far more absorption lines than emission lines for each of these new molecular species. Hence, it is important to understand the nature, distribution, and intensity of the underlying continuum in the GBT bandpasses for the purposes of radiative transfer, i.e., the means by which reliable molecular abundances are estimated. We find that the GBT spectrometer bandpass continuum is consistent with optically thin, nonthermal (synchrotron) emission with a flux density spectral index of  $-0.7$  and a Gaussian source size of  $\sim 143''$  at 1 GHz that decreases with increasing frequency as  $\nu^{-0.52}$ . Some support for this model is provided by high-frequency VLA observations of Sgr B2.

*Subject headings:* H II regions — ISM: individual (Sagittarius B2(N-LMH)) — radiation mechanisms: nonthermal — radio continuum: ISM

The north source in Sgr B2, i.e., Sgr B2(N), is a giant star-forming region that lies along the Galactic equator near the center of our Galaxy. There is another strong molecular source  $\sim 60''$  to the south of this position known as the main in Sgr B2, i.e., Sgr B2(M), that can influence molecular detections toward Sgr B2(N) if the telescope beam is large. Both Sgr B2(N) and Sgr B2(M) contain molecular maser-emitting spots, ultracompact H II continuum sources, compact hot molecular cores of arcsecond dimensions, extended H II regions, and cold extended molecular regions of arcminute dimensions. In addition, small-scale and large-scale shock phenomena pervade this region (e.g., Chengalur & Kanekar 2003). In Sgr B2(N), the hot molecular core known as the LMH (Large Molecule Heimat) has been a primary source that has been searched for millimeter-wave rotational transitions between high-energy levels for species that are found in emission and confined to its  $\sim 5''$  diameter. For example, from interferometric observations, the emission from high-energy transitions of methyl formate ( $\text{CH}_3\text{OCHO}$ ; Mehringer et al. 1997), acetic acid ( $\text{CH}_3\text{COOH}$ ; Mehringer et al. 1997), ethyl cyanide ( $\text{CH}_3\text{CH}_2\text{CN}$ ; Miao & Snyder 1997), formic acid ( $\text{HCOOH}$ ; Liu et al. 2001), and acetone ( $\text{CH}_3\text{COCH}_3$ ; Snyder et al. 2002) is seen largely confined to the LMH core. High-energy transitions of methanol ( $\text{CH}_3\text{OH}$ ) are also confined to the LMH hot core, and they were used by Pei et al. (2000) to derive a rotational temperature of  $170 \pm 13$  K that is usually assumed to characterize other large molecules in the core.

On the other hand, recent observations with the Green Bank Telescope (GBT) toward Sgr B2(N-LMH) indicate that the molecular halo surrounding the LMH is a rich source of an entirely different set of large complex molecules. In this cold halo region, transitions between low-energy levels of large interstellar molecules tend to occur in the frequency range 1–48 GHz. For example, glycolaldehyde ( $\text{CH}_2\text{OHCHO}$ ) was first detected in this region with the GBT by means of the  $1_{10}-1_{01}$ ,  $2_{11}-2_{02}$ ,  $3_{12}-3_{03}$ , and  $4_{13}-4_{04}$  rotational transitions at 13.48, 15.18, 17.98, and 22.14 GHz, respectively; all levels involved in these four transitions have energies less than 6.5 K. Only the  $1_{10}-1_{01}$  transition of glycolaldehyde was seen

solely in emission; all the other transitions were seen predominantly in absorption. An analysis of these four rotational transitions yields a glycolaldehyde state temperature of  $\sim 8$  K (Hollis et al. 2004a) that is probably characteristic of the cold halo region surrounding the LMH. Other large molecules that have been detected predominantly in absorption toward Sgr B2(N-LMH) with the GBT by means of transitions between low-energy levels include propenal ( $\text{CH}_2\text{CHCHO}$ ; Hollis et al. 2004b), propanal ( $\text{CH}_3\text{CH}_2\text{CHO}$ ; Hollis et al. 2004b), acetamide ( $\text{CH}_3\text{CONH}_2$ ; Hollis et al. 2006a), and cyclopropanone ( $c\text{-H}_2\text{C}_3\text{O}$ ; Hollis et al. 2006b). It is important to note that other molecular sources observed with the GBT, such as the dark cloud TMC-1 or the IRC +10°216 circumstellar nebula, show no measurable continuum in the spectrometer bandpass. However, low-energy transitions of  $\text{H}_2\text{CO}$  (e.g.,  $1_{11}-1_{10}$ ) in TMC-1 have been observed to exhibit absorption against the cosmic background (Palmer et al. 1969). It is also noteworthy that the GBT detection of ketenimine ( $\text{CH}_2\text{CNH}$ ; Lovas et al. 2006) in absorption toward Sgr B2(N-LMH) suggests that an intermediate-temperature region is responsible because the transitions involved are between intermediate-energy levels that range from 33 to 51 K.

As a consequence of our deep integration observations in search of new molecules, extensive low noise level data have been collected in 85 spectrometer bandpasses centered at different frequencies in the range of 1–48 GHz. The continuum antenna temperature in each spectrometer bandpass is observed to be a function of bandpass center frequency, thus providing the means for analyzing the source of continuum reported here.

Spectral line observations over the range of 1–48 GHz were conducted with the NRAO<sup>4</sup> 100 m Robert C. Byrd GBT from 2004 March 4 to 2005 November 12. The GBT spectrometer was configured to provide four intermediate-frequency (IF) bandwidths at a time in two polarizations through the use of offset oscillators in the IF. In the six columns of Table 1, we list the receiver band, the receiver tuning range, the spectrometer bandwidth per IF, the spectrometer channel spacing, and 2004 and 2005 observation dates, respectively. GBT half-power beamwidths can be approximated by

$$\theta_B \approx 740''/\nu, \quad (1)$$

<sup>1</sup> NASA Goddard Space Flight Center, Computational and Information Sciences and Technology Office, Greenbelt, MD 20771.

<sup>2</sup> National Radio Astronomy Observatory, Charlottesville, VA 22903-2475.

<sup>3</sup> Optical Technology Division, National Institute of Standards and Technology, Gaithersburg, MD 20899.

<sup>4</sup> The National Radio Astronomy Observatory is a facility of the NSF, operated under cooperative agreement by Associated Universities, Inc.

TABLE 1  
OBSERVATIONAL PARAMETERS

Band	Receiver (GHz)	IF Bandwidth (MHz)	Resolution (kHz)	Obs. Dates (2004)	Obs. Dates (2005)
L	1.15–1.73	50	6.1	...	Sep 9
S	1.73–2.60	50	6.1	...	Sep 8
C	3.95–5.85	200	24.4	...	Sep 28; Oct 9–11
X	8.00–10.1	200	24.4	...	Sep 6, 18, 19; Nov 10
Ku	12.00–15.4	200	24.4	Mar 4; Apr 17	Sep 7, 14, 22
K	18.00–22.4	200	24.4	Feb 25, 29; Mar 13, 29; Apr 5, 6, 15	Apr 1; Nov 12
	22.00–26.5	200	24.4	Mar 10; Apr 16	Oct 11–14
Q	40.00–48.0	800	390.7	...	Mar 14, 15, 19, 22, 30, 31; Apr 5

where the observing frequency ( $\nu$ ) is in units of GHz. Over the course of the observations, the spectrometer bandpasses were centered at a total of 85 different frequencies in the range of 1.35–47.68 GHz that correspond to  $\theta_B \approx 548''$  and  $\theta_B \approx 16''$ , respectively. The Sgr B2(N-LMH) J2000 pointing position employed was  $\alpha = 17^{\text{h}}47^{\text{m}}19.8^{\text{s}}$ ,  $\delta = -28^{\circ}22'17''$ , which correspond to Galactic coordinates of  $l = 0.6775^{\circ}$ ,  $b = -0.0271^{\circ}$ . An LSR source velocity of  $+64 \text{ km s}^{-1}$  was assumed. Spectrometer data were taken in the OFF-ON position-switching mode, with the OFF position  $60'$  east in azimuth with respect to the ON-source position. A single scan consisted of 2 minutes in the OFF-source position followed by 2 minutes in the ON-source position. Sgr B2(N-LMH) was observed in this manner above  $10^{\circ}$  elevation from source rise to source set (i.e., a 6 hr track). Note that at ON-source transit, the OFF-source position in Galactic coordinates is  $l = 1.205^{\circ}$ ,  $b = -0.876^{\circ}$ , and all OFF positions along the 6 hr track are well clear of sources of contamination. The accumulated scans over two or three tracks for the two polarization outputs from the spectrometer were averaged in the final data reduction process. The antenna temperatures of the spectral line and continuum emission produced in the spectrometer bandpass are on the  $T_A^*$  scale (Ulich & Haas 1976) with estimated 20% uncertainties.

The instrumental slope in a GBT spectrometer bandpass can be quite significant in the presence of source continuum emission (see Fig. 3 of Hollis 2006), and there can be unpredictable effects at the edges of the bandpass. Therefore, a continuum antenna

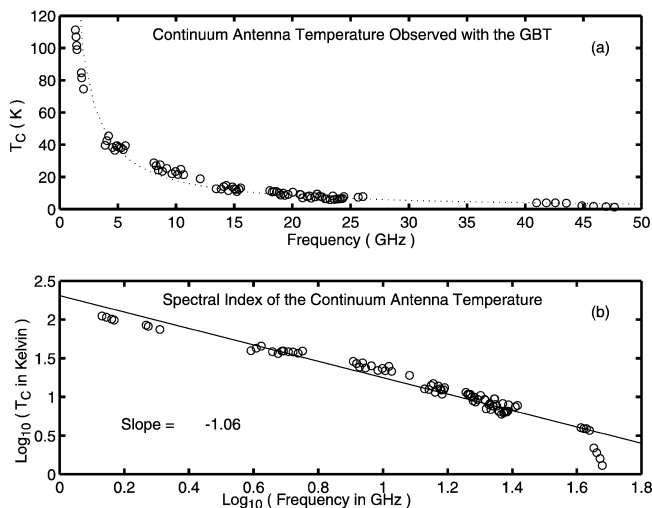


FIG. 1.—Continuum antenna temperatures observed with the GBT spectrometer toward Sgr B2(N-LMH). Panel *a* plots continuum antenna temperature as a function of spectrometer bandpass center frequency. Panel *b* is a log-log plot of panel *a* data. A linear least-squares fit to panel *b* data yields a slope of  $-1.06$  that determines the spectral index of the continuum antenna temperature. The dotted line in panel *a* is the result from the fit to data in panel *b*.

temperature ( $T_C$ ) was estimated at or near the center of each of the 85 different spectrometer bandpasses. Figure 1*a* is a linear-linear plot of  $T_C$  versus spectrometer bandpass center frequency, and Figure 1*b* is a log-log plot of the same data. The  $-1.06$  slope of Figure 1*b* was determined by a linear least-squares fit and represents the spectral index of  $T_C$ . The fit result is superimposed as a dotted line on Figure 1*a*. These plots show that  $T_C$  is a highly predictable function of frequency for GBT spectrometer bandpasses in the range of 1–48 GHz. The main-beam brightness temperature ( $T_B$ ) is determined from  $T_C$  divided by the GBT beam efficiency, which can be estimated by

$$\eta_B = -15.52 \times 10^{-5} \nu^2 - 22.59 \times 10^{-4} \nu + 0.98, \quad (2)$$

where  $\nu$  is in the range of 1.35–47.68 GHz that corresponds to  $\eta_B \approx 0.97$  and  $\eta_B \approx 0.53$ , respectively. Equation (2) derives from a fit to the Ruze (1966) formulation, assuming a GBT surface accuracy of  $390 \mu\text{m}$  and an aperture efficiency  $\eta_A(\nu = 0) = 0.71$ , and favorably compares with similar results in Langston & Turner (2007). Figure 2*a* is a log-log plot of  $T_B$  as a function of the center frequency in the 85 spectrometer bandpasses. The  $-0.94$  slope of Figure 2*a* was determined by a linear-least squares fit and represents the spectral index of  $T_B$ . In what follows, we develop a method for estimating the spectral index of the flux density ( $S$ ) of the observed continuum that influences

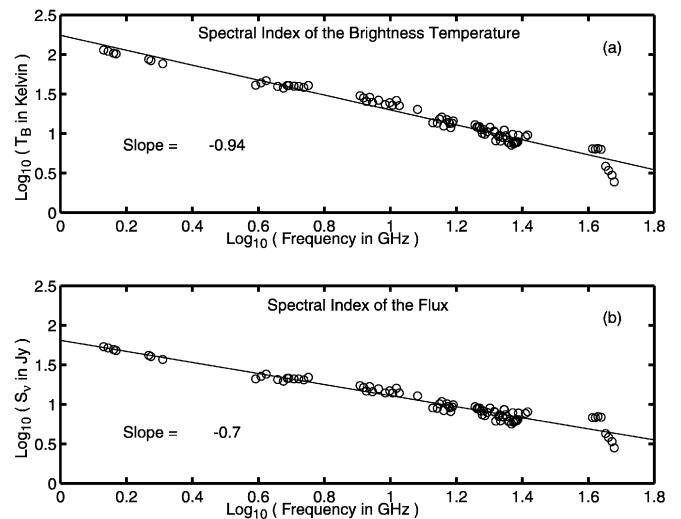


FIG. 2.—Spectral indices of the brightness temperature and flux density observed with the GBT spectrometer toward Sgr B2(N-LMH). Panel *a* is a log-log plot of the brightness temperature as a function of bandpass center frequency. The resultant slope of  $-0.94$  determines the spectral index of the brightness temperature. Panel *b* is a log-log plot of the observed flux density as a function of bandpass center frequency that is dependant on the observed source size (see text). The resultant slope of  $-0.7$  determines the spectral index of the flux density, suggesting that the source of continuum is optically thin and nonthermal.

TABLE 2  
CONTINUUM SOURCE SIZE ( $\theta_s$ ) ESTIMATES

Frequency (GHz)	Taper FWHM (arcsec)	Convolved Source $\theta(\text{maj}) \times \theta(\text{min})$ (arcsec)	VLA Beam $\theta(\text{maj}) \times \theta(\text{min})$ (arcsec)	$\theta_s$ (arcsec)	Sgr B2 Component
4.86	152	215.3 $\times$ 101.9	150.2 $\times$ 119.5	63.2	North+Main
22.15	33	36.8 $\times$ 30.5 36.9 $\times$ 30.1	33.4 $\times$ 26.4	15.5 15.1	North Main
43.75	17	26.4 $\times$ 13.7 19.1 $\times$ 7.6	23.1 $\times$ 10.5	10.9 ...	North Main

NOTE.—Derived from VLA restoring beams that approximate corresponding GBT beam sizes (see text and eq. [4]).

the bandpass shape. The value of the spectral index of  $S$  is an indication of the nature of the continuum emission itself.

A spectral index ( $\alpha$ ) of a source can be cast in terms of its continuum antenna temperature ( $T_C$ ), its brightness temperature ( $T_B$ ), or its flux density ( $S$ ), each of which has a value proportional to  $\nu^\alpha$ . The spectral indices for  $T_C$ ,  $T_B$ , and  $S$  will, in general, have different numerical values, and they are related through the following equation for the flux density of an unmapped source:

$$S = 2k \frac{\nu^2}{c^2} \frac{\pi \theta_B^2}{4 \ln 2} T_B (1 + \theta_s^2 / \theta_B^2), \quad (3)$$

where  $k$  is the Boltzmann constant,  $c$  is the speed of light,  $\theta_B$  is the Gaussian half-power beamwidth,  $\theta_s$  is an intrinsic Gaussian source size,  $\pi \theta_B^2 / 4 \ln 2$  is the main-beam solid angle for a Gaussian pattern, and the term in parentheses accounts for the source extending beyond the telescope beam ( $\theta_s > \theta_B$ ). Note that the term in parentheses approaches unity when the source is much smaller than the beam. To calculate the flux density as a function of frequency in equation (3), we must have an independent measure of the source size that may also be a function of frequency.

To estimate the intrinsic, deconvolved source size ( $\theta_s$ ), we used Very Large Array (VLA) archival data taken at observing frequencies of 4.86, 22.15, and 43.75 GHz toward the molecular pointing position Sgr B2(N-LMH). It was necessary to taper these VLA data in the MIRIAD task INVERT to approximate GBT beam sizes of 152", 33", and 17" at 4.86, 22.15, and 43.75 GHz, respectively. The "true" source size ( $\theta_s$ ) is assumed to be related to the observed source size ( $\theta_{\text{OBS}}$ ) and the VLA beam ( $\theta_{\text{VLA}}$ ) by

$$\theta_{\text{OBS}}(\text{maj}) \times \theta_{\text{OBS}}(\text{min}) = \theta_{\text{VLA}}(\text{maj}) \times \theta_{\text{VLA}}(\text{min}) + \theta_s^2. \quad (4)$$

We note that despite tapering the VLA visibility data, some

diffuse emission may still be resolved out, introducing an unknown systematic uncertainty into equation (4). The VLA results in Table 2 are the observing frequency, the taper (i.e., the FWHM parameter set in the MIRIAD task INVERT) used to approximate the GBT beam, the convolved source size from a Gaussian fit, the VLA restoring beam size, the source size resulting from equation (4), and the Sgr B2 component detected. The most obvious result from Table 2 is that the larger telescope beam at 4.86 GHz fails to resolve the two major components of continuum at the Sgr B2(N) and Sgr B2(M) positions. The left side of Figure 3 shows the observed source size overlaid on a gray-scale image of the 4.86 GHz continuum; the right side shows the deconvolved source size within the 152" diameter GBT beam. By comparison, Figure 4 shows the results for 22.15 GHz in which the two major components Sgr B2(N) and Sgr B2(M) are resolved.

The intrinsic source size for the north component decreases with increasing frequency, as shown in Table 2. Based on the 22.15 and 43.75 GHz entries in Table 2, we calculate that  $\theta_s$  (north only) =  $77'' \nu^{-0.52}$ , where the observed frequency ( $\nu$ ) is in units of GHz. If the same frequency dependence is assumed for all sources of the continuum encompassed in larger telescope beams (e.g., at 4.86 GHz), then the following frequency relation for the effective size of all sources of continuum is obtained:

$$\theta_s \approx 143'' (\nu)^{-0.52}, \quad (5)$$

which yields  $\theta_s = 62.8''$  for an observing frequency of 4.86 GHz, in agreement with the corresponding Table 2 entry in which the continuum components are unresolved.

Using the brightness temperature data from Figure 2a and the estimate of the source size given by equation (5), the flux density  $S$  as a function of frequency is computed by means of

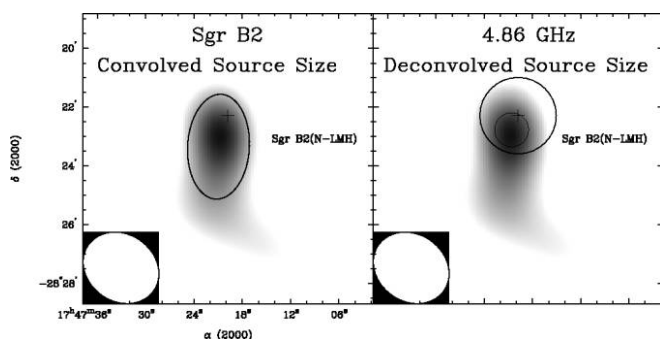


FIG. 3.—VLA observations of Sgr B2 at 4.86 GHz. These VLA observations were processed to approximate the GBT beam (see text and Table 2). The left side shows the observed source size overlaid on a gray-scale image of the 4.86 GHz continuum; the right side shows the deconvolved source size within the 152" diameter GBT beam. Note that the primary sources of continuum [i.e., Sgr B2(N) and Sgr B2(M)] are unresolved.

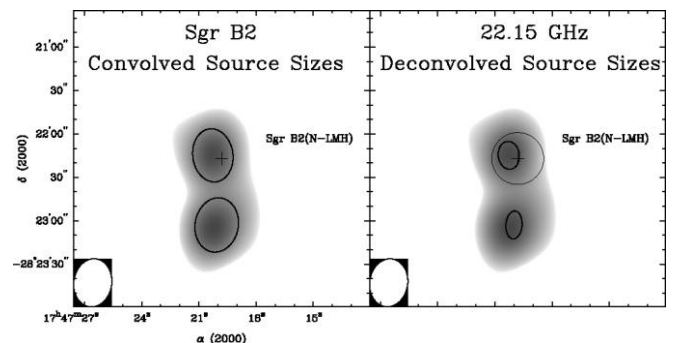


FIG. 4.—VLA observations of Sgr B2 at 22.15 GHz. These VLA observations were processed to approximate the GBT beam (see text and Table 2). The left side shows the observed source size overlaid on a gray-scale image of the 22.15 GHz continuum; the right side shows the deconvolved source size within the 33" diameter GBT beam. Note that the primary sources of continuum [i.e., Sgr B2(N) and Sgr B2(M)] are resolved.

equation (3). Figure 2*b* is a log-log plot of  $S$ . The  $-0.7$  slope of Figure 2*b* was determined by a linear least-squares fit and represents the spectral index of  $S$ . Since the slope of Figure 2*b* is negative and quite linear, showing no indication of turnover at lower frequency, these data are consistent with a synchrotron spectrum from a power-law distribution of electrons in the optically thin case (see Fig. 6.12 of Rybicki & Lightman 1979).

When the GBT is pointed toward Sgr B2(N-LMH), the 1–48 GHz continuum detected in the spectrometer bandpass is consistent with an optically thin, nonthermal source. Moreover, this pointing position is toward the K2 ultracompact H II region with other thermal sources in its vicinity; these smaller thermal sources would be severely beam-diluted in the present GBT observations. It has been long known that there is a continuous distribution of background continuum radiation from our Galaxy composed of a thermal spectrum and a nonthermal spectrum with maximum intensity toward the plane (e.g., Kraus 1966). Moreover, Yusef-Zadeh et al. (2003) have reported nonthermal emission specifically near the Galactic center, and Sofue (1994) has argued that the radio continuum from the  $3^\circ \times 3^\circ$  Galactic center region is a mixture of synchrotron and free-free emissions. Thus, the results in this work are consistent with a mixture of thermal and nonthermal radio emission expected since Sgr B2 lies along the Galactic equator near the Galactic center. Furthermore, nonthermal emission toward Sgr B2 at frequencies lower than 1.5 GHz has been observed (F. Yusef-Zadeh 2007, private communication). Moreover, Yusef-Zadeh et al. (2007) report a low-energy cosmic-ray model that predicts a nonthermal radio spectrum, and Crocker et al. (2007) suggest that secondary electrons from  $\gamma$ -rays could produce nonthermal radio emission in Sgr B2.

In particular, Sgr B2(N) and its many sources of continuum emission have been previously well studied with the VLA, albeit at higher spatial resolution than the GBT spectrometer data presented here. For example, Gaume et al. (1995, Fig. 10) produced a  $2.7''$  resolution spectral index image of the flux density from continuum images at 1.5 and 22.3 GHz. The locations of ultracompact H II regions show up prominently with a spectral index of the flux density  $\sim 1$  (i.e., the slope), indicating optically thick thermal emission from dust and/or emission primarily from free-free radiation. Similarly, Mehringer & Menten (1997, Fig. 2) produced a  $\sim 3''$  resolution spectral index image from 8.4 and 44 GHz data, showing that the spectral index of the flux density is  $\sim 0.8$  toward the ultracompact H II region K2; however, northeast of K2 (at  $\sim 3''$  resolution and

over an area with a scale size of  $\sim 20''$ ) the spectral index of the flux density is largely zero, indicating optically thin thermal emission of an extended but clumpy H II region. Moreover, Mehringer & Menten (1997) obtain a 44 GHz thermal continuum flux density of 5.5 Jy for Sgr B2(N) from high-resolution VLA observations, while we obtain 4.6 Jy at 44 GHz for the nonthermal continuum flux density in low-resolution GBT observations reported here. These flux density results are disparate and mutually exclusive because of missing short antenna spacings in the VLA observations that are needed to detect the large-scale spatial component that the GBT samples well. It is interesting to note that Akabane et al. (1988) compared matched  $\sim 40''$  resolution observations of the Effelsberg 100 m telescope at 23 GHz and the Nobeyama 45 m telescope at 43 GHz to conclude that Sgr B2 is largely thermal. At both frequencies, they obtain an observed source scale size of  $\sim 45''$  toward both Sgr B2(N) and Sgr B2(M), suggesting that the source size is not a function of frequency. Thus, it is likely that the Akabane et al. (1988) methodology samples different gas than that gas sampled by the GBT spectrometer at 85 different frequencies, further confirming that disentangling thermal and nonthermal emission is often a vexing problem.

In summary, an analysis of continuum antenna temperatures detected in the GBT spectrometer bandpasses is presented for observations toward Sgr B2(N-LMH). The continuum controls the absorption features seen in molecular absorption transitions between low-energy levels of several new complex molecules observed with the GBT and therefore influences estimates of molecular abundances. The analysis herein assesses the nature and the effective scale size of the continuum source observed within the GBT spectrometer bandpasses centered on different frequencies. The methodology employed determines the spectral indices of the continuum antenna temperature and the brightness temperature across all spectrometer bandpasses, determines the source size as a function of frequency from archival VLA data, and then estimates the spectral index of the flux density. As a result, the GBT spectrometer bandpass continuum seen toward Sgr B2(N-LMH) is consistent with optically thin, nonthermal (synchrotron) emission with a flux density spectral index of  $-0.7$  and a Gaussian source size of  $\sim 143''$  at 1 GHz that decreases with increasing frequency as  $\nu^{-0.52}$ .

We thank Ed Churchwell, Farhad Yusef-Zadeh, Michael Remijan, and an anonymous reviewer for helpful comments.

#### REFERENCES

- Akabane, K., Sofue, Y., Hirabayashi, H., Morimoto, M., Inoue, M., & Downes, D. 1988, *PASJ*, 40, 459
- Chengalur, J. N., & Kanekar, N. 2003, *A&A*, 403, L43
- Crocker, R. M., Jones, D., Protheroe, R. J., Ott, J., Ekers, R., Melia, F., Stanev, T., & Green, A. 2007, *ApJ*, submitted (astro-ph/0702045)
- Gaume, R. A., Claussen, M. J., De Pree, C. G., Goss, W. M., & Mehringer, D. M. 1995, *ApJ*, 449, 663
- Hollis, J. M. 2006, in *IAU Symp. 231, Astrochemistry: Recent Successes and Current Challenges*, ed. D. C. Lis, G. A. Blake, & E. Herbst (Cambridge: Cambridge Univ. Press), 227
- Hollis, J. M., Jewell, P. R., Lovas, F. J., & Remijan, A. J. 2004a, *ApJ*, 613, L45
- Hollis, J. M., Jewell, P. R., Lovas, F. J., Remijan, A. J., & Møllendal, H. 2004b, *ApJ*, 610, L21
- Hollis, J. M., Lovas, F. J., Remijan, A. J., Jewell, P. R., Ilyushin, V. V., & Kleiner, I. 2006a, *ApJ*, 643, L25
- Hollis, J. M., Remijan, A. J., Jewell, P. R., & Lovas, F. J. 2006b, *ApJ*, 642, 933
- Kraus, J. D. 1966, *Radio Astronomy* (New York: McGraw-Hill)
- Langston, G., & Turner, B. 2007, *ApJ*, 658, 455
- Liu, S.-Y., Mehringer, D. M., & Snyder, L. E. 2001, *ApJ*, 552, 654
- Lovas, F. J., Hollis, J. M., Remijan, A. J., & Jewell, P. R. 2006, *ApJ*, 645, L137
- Mehringer, D. M., & Menten, K. M. 1997, *ApJ*, 474, 346
- Mehringer, D. M., Snyder, L. E., Miao, Y., & Lovas, F. J. 1997, *ApJ*, 480, L71
- Miao, Y., & Snyder, L. E. 1997, *ApJ*, 480, L67
- Palmer, P., Zuckerman, B., Buhl, D., & Snyder, L. E. 1969, *ApJ*, 156, L147
- Pei, C. C., Liu, S.-Y., & Snyder, L. E. 2000, *ApJ*, 530, 800
- Ruze, J. 1966, *Proc. IEEE*, 54, 633
- Rybicki, G. B., & Lightman, A. P. 1979, *Radiative Processes in Astrophysics* (New York: Wiley)
- Sofue, Y. 1994, in *The Nuclei of Normal Galaxies*, ed. R. Genzel & A. I. Harris (NATO ASI Ser. C, 445; Dordrecht: Kluwer), 43
- Snyder, L. E., Lovas, F. J., Mehringer, D. M., Miao, N. Y., Kuan, Y.-J., Hollis, J. M., & Jewell, P. R. 2002, *ApJ*, 578, 245
- Ulich, B. L., & Haas, R. W. 1976, *ApJS*, 30, 247
- Yusef-Zadeh, F., Muno, M., Wardle, M., & Lis, D. C. 2007, *ApJ*, 656, 847
- Yusef-Zadeh, F., Nord, M., Wardle, M., Law, C., Lang, C., & Lazio, T. J. W. 2003, *ApJ*, 590, L103